catalysts

Electronic Supplementary Information

Density Functional Theory Study of CuAg Bimetal Electrocatalyst for CO_2RR to Produce CH_3OH

Sensen Xue [1], Xingyou Liang [1], Qing Zhang [1], Xuefeng Ren [2], Liguo Gao [1], Tingli Ma [3,4] and Anmin Liu [1,*]

[1] State Key Laboratory of Fine Chemicals, School of Chemical Engineering, Dalian University of Technology, Dalian 116081, China; xuess@mail.dlut.edu.cn (S.X.)
[2] School of Ocean Science and Technology, Dalian University of Technology, Panjin 124221, China
[3] Department of Materials Science and Engineering, China Jiliang University, Hangzhou 310018, China; tinglima@life.kyutech.ac.jp
[4] Graduate School of Life Science and Systems Engineering, Kyushu Institute of Technology, 2-4 Hibikino, Wakamatsu, Kitakyushu 808-0196, Fukuoka, Japan
* Correspondence: liuanmin@dlut.edu.cn

Table S1. The energy of Ag_3 clusters.

isomers	E_{Ag3}/Ha	E_B/Ha
straight	-15598.809	-0.100
triangle	-15598.810	-0.100

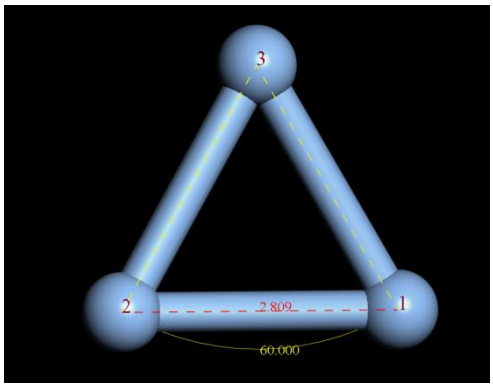

Figure S1. The most stable structure of Ag_3 clusters.

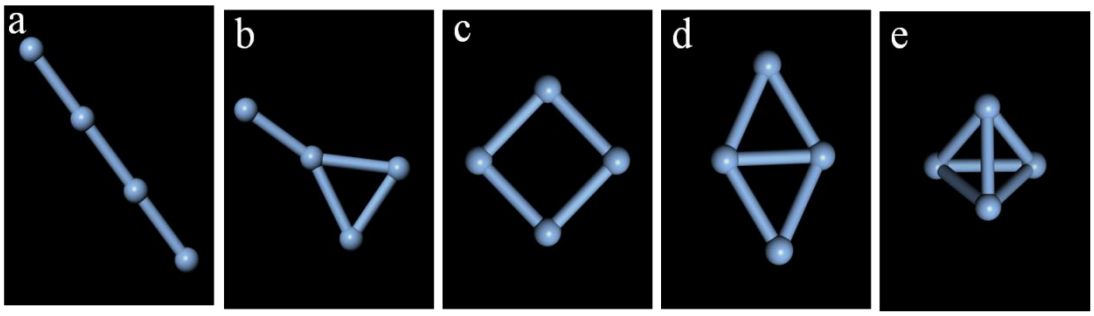

Figure S2. The isomeric structure of Ag_4 clusters.

Table S2. The energy of Ag_4 clusters.

isomers	E_{Ag4}/Ha	E_B/Ha
a	-20798.427	-0.147
b	-20798.444	-0.165
c	-20798.426	-0.146
d	-20798.449	-0.169
e	-20798.417	-0.138

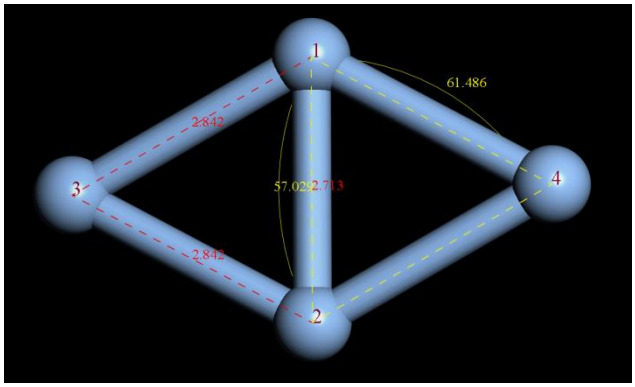

Figure S3. The most stable structure of Ag_4 clusters.

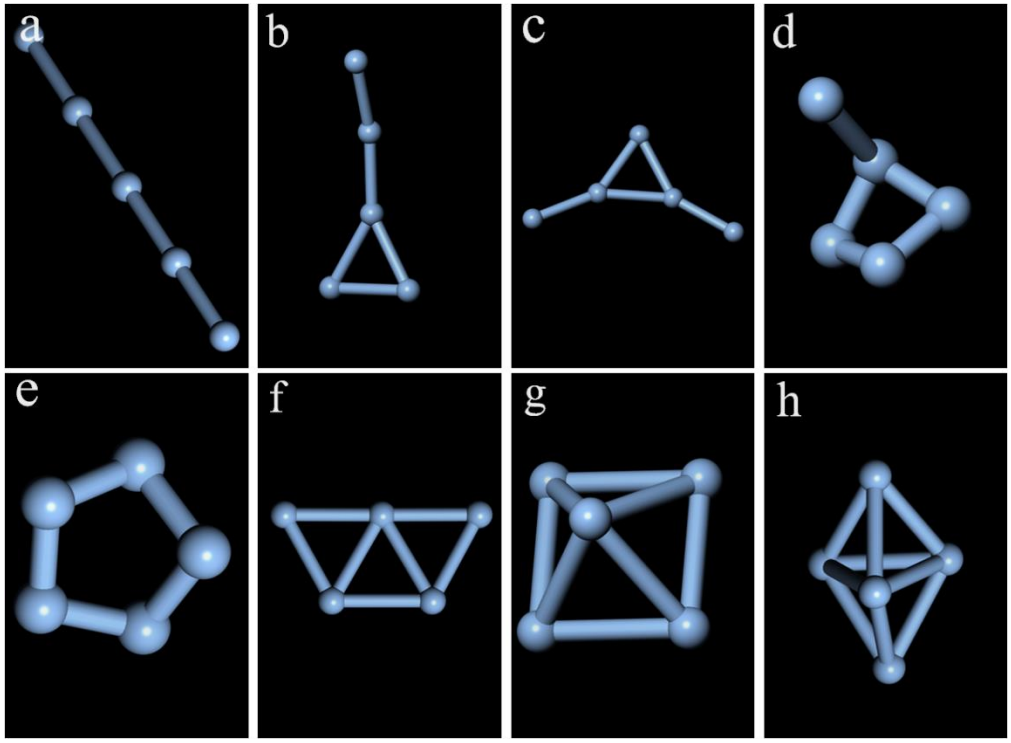

Figure S4. The isomeric structure of Ag_5 clusters.

Table S3. The energy of Ag_5 clusters.

isomers	E_{Ag5}/Ha	E_B/Ha
a	-25998.036	-0.187
b	-25998.050	-0.201
c	-25998.053	-0.204
d	-25998.064	-0.215
e	-25998.065	-0.215
f	-25998.080	-0.231
g	-25998.061	-0.211
h	-25998.065	-0.215

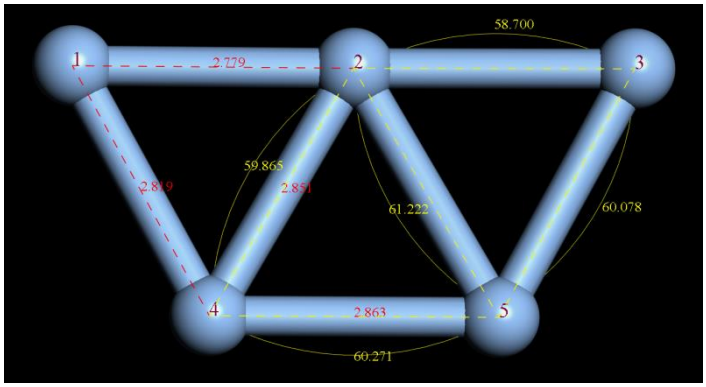

Figure S5. The most stable structure of Ag_5 clusters.

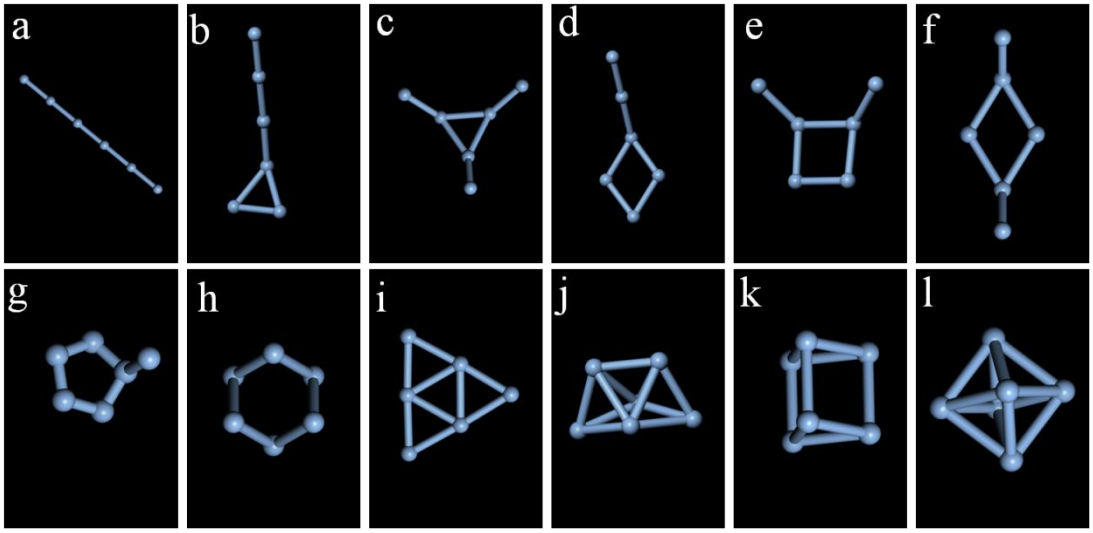

Figure S6. The isomeric structure of Ag_6 clusters.

Table S4. The energy of Ag_6 clusters.

isomers	E_{Ag6}/Ha	E_B/Ha
a	-31197.650	-0.232
b	-31197.671	-0.252
c	-31197.679	-0.261
d	-31197.662	-0.243
e	-31197.692	-0.273
f	-31197.673	-0.254
g	-31197.677	-0.258
h	-31197.724	-0.305
i	-31197.698	-0.279
j	-31197.729	-0.310
k	-31197.698	-0.279
l	-31197.688	-0.269

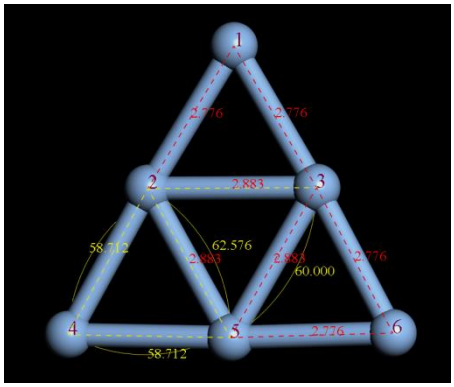

Figure S7. The most stable structure of Ag_6 clusters.

Table S5. The average binding energy of Ag_n (n=1~6) clusters.

n	E_B / eV	E_b / eV
1	0	0
2	-1.776	-0.888
3	-2.726	-0.909
4	-4.606	-1.152
5	-6.290	-1.258
6	-8.441	-1.407

Table S6. The energy of Cu_1Ag_5 clusters.

isomers	E_{CuAg}/Ha	E_B/Ha	E_B/eV	E_b/eV
a	-27638.468	-0.329	-8.964	-1.494
b	-27638.464	-0.325	-8.850	-1.475

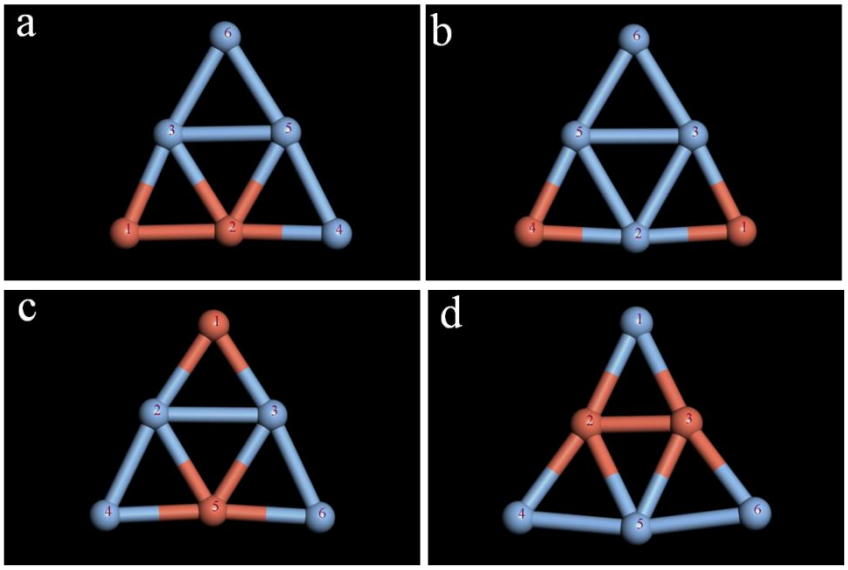

Figure S8. The isomeric structure of Cu_2Ag_4 clusters.

Table S7. The energy of Cu_2Ag_4 clusters.

isomers	E_{CuAg}/Ha	E_B/Ha	E_B/eV	E_b/eV
a	-24079.204	-0.346	-9.418	-1.570
b	-24079.198	-0.340	-9.255	-1.542
c	-24079.201	-0.344	-9.365	-1.561
d	-24079.208	-0.351	-9.541	-1.590

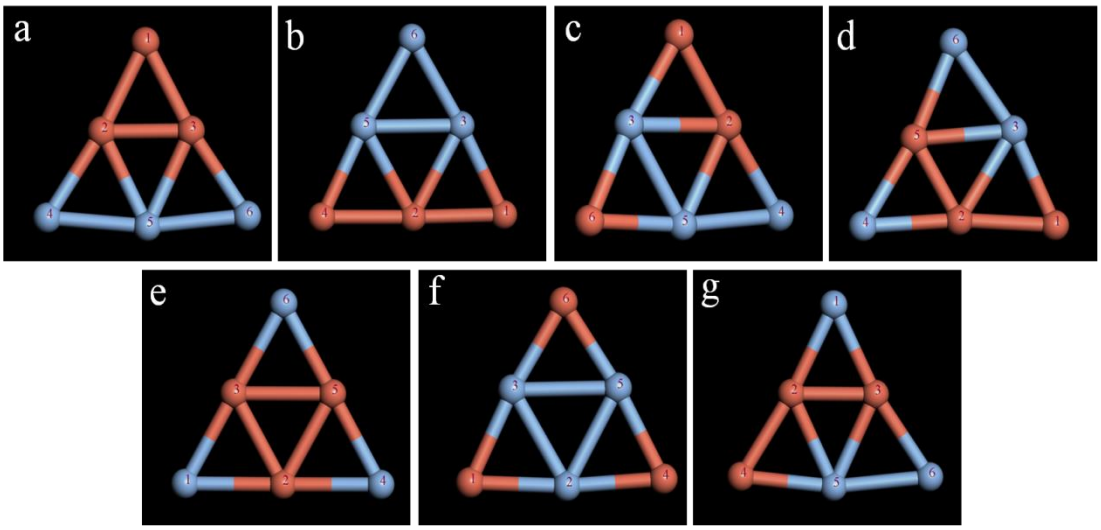

Figure S9. The isomeric structure of Cu_3Ag_3 clusters.

Table S8. The energy of Cu_3Ag_3 clusters.

isomers	E_{CuAg}/Ha	E_B/Ha	E_B/eV	E_b/eV
a	-20519.939	-0.362	-9.860	-1.643
b	-20519.946	-0.369	-10.033	-1.672
c	-20519.943	-0.367	-9.978	-1.663
d	-20519.937	-0.360	-9.807	-1.635
e	-20519.932	-0.355	-9.656	-1.609
f	-20519.950	-0.373	-10.153	-1.692
g	-20519.943	-0.367	-9.978	-1.663

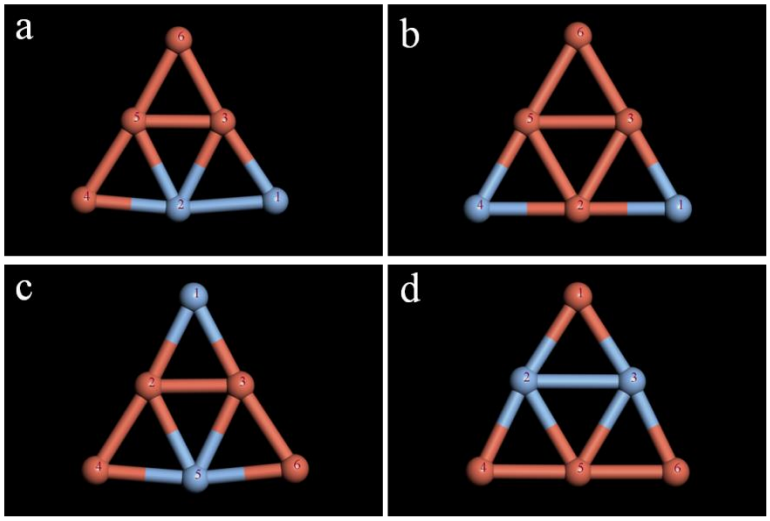

Figure S10. The isomeric structure of Cu_4Ag_2 clusters.

Table S9. The energy of Cu_4Ag_2 clusters.

isomers	E_{CuAg}/Ha	E_B/Ha	E_B/eV	E_b/eV
a	-16960.680	-0.384	-10.460	-1.743
b	-16960.687	-0.391	-10.633	-1.772
c	-16960.679	-0.383	-10.408	-1.735
d	-16960.673	-0.377	-10.247	-1.708

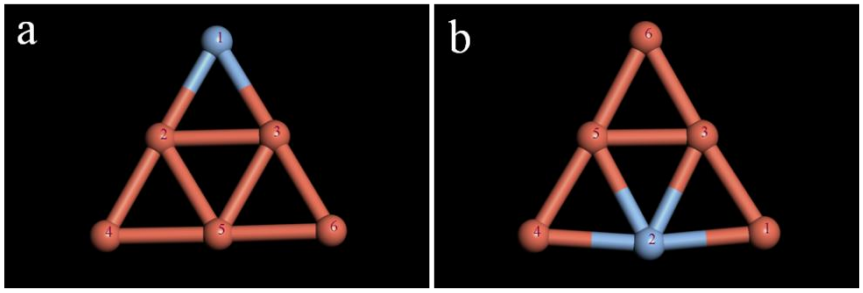

Figure S11. The isomeric structure of Cu_5Ag_1 clusters.

Table S10. The energy of Cu_5Ag_1 clusters.

isomers	E_{CuAg}/Ha	E_B/Ha	E_B/eV	E_b/eV
a	-13401.423	-0.408	-11.099	-1.850
b	-13401.415	-0.400	-10.882	-1.814

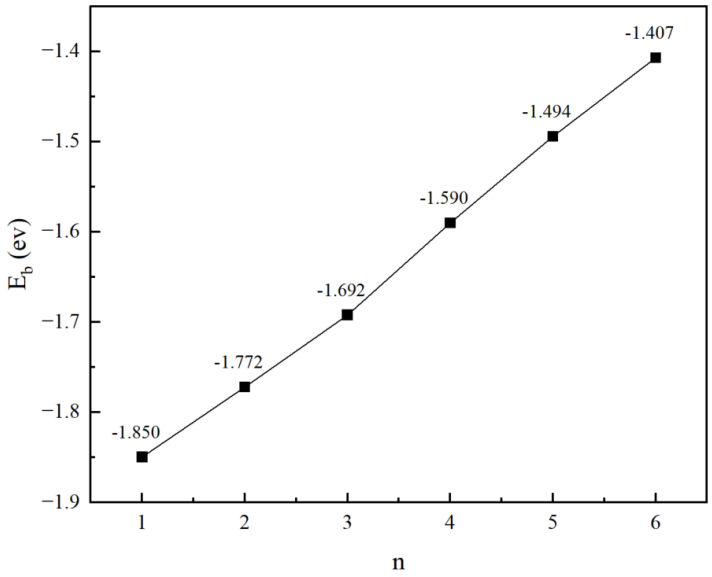

Figure S12. The change of average binding energy of $Cu_{6-n}Ag_n$ clusters with n.

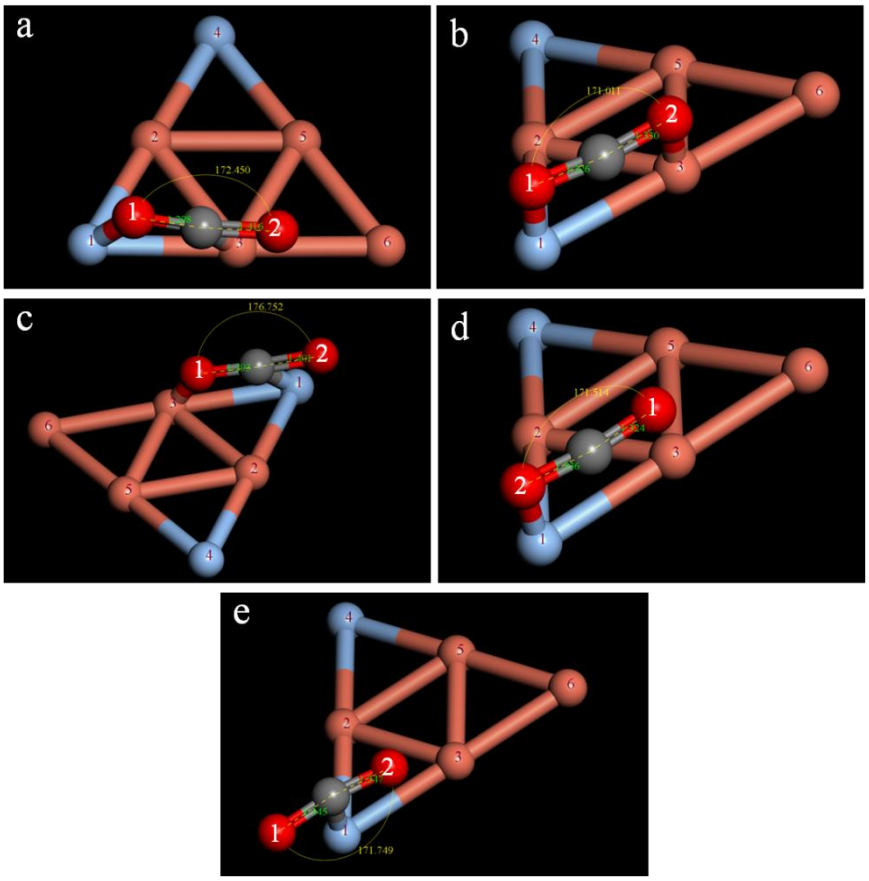

Figure S13. The isomers of the Cu_4Ag_2-CO_2 adsorption structure.

Table S11. Bond length, bond angle and energy of Cu_4Ag_2-CO_2 structure.

isomers	∠O1CO2/°	$d_{C\text{-}O1}$/Å	$d_{C\text{-}O2}$/Å	$E_{CuAg\text{-}CO2}$/Ha	E_{obs}/eV
a	172.450°	1.298	1.416	-17149.166	-0.0698
b	171.011°	1.326	1.330	-17149.166	-0.079
c	176.752°	1.293	1.401	-17149.174	-0.288
d	171.514°	1.324	1.336	-17149.167	-0.096
e	171.749°	1.345	1.347	-17149.174	-0.287

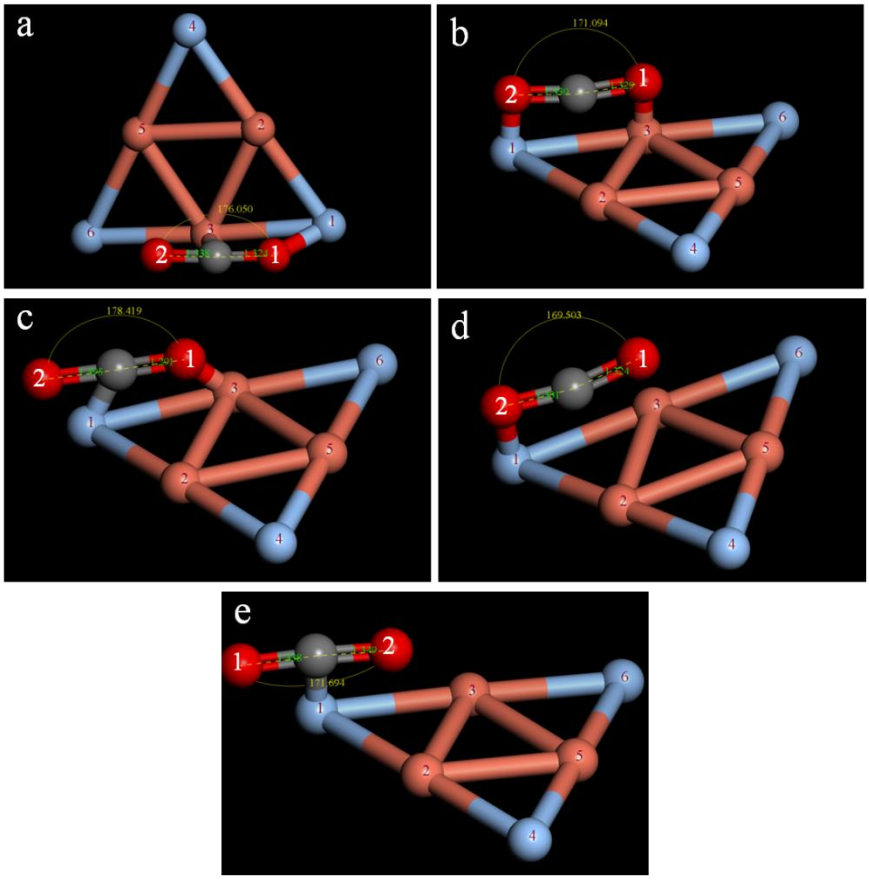

Figure S14. The isomers of the Cu_3Ag_3-CO_2 adsorption structure.

Table S12. Bond length, bond angle and energy of Cu_3Ag_3-CO_2 structure.

isomers	∠O1CO2/°	$d_{C\text{-}O1}$/ Å	$d_{C\text{-}O2}$/ Å	$E_{CuAg\text{-}CO2}$/Ha	E_{obs}/eV
a	176.050°	1.324	1.338	-20708.431	-0.140
b	171.094°	1.329	1.330	-20708.429	-0.058
c	178.419°	1.291	1.395	-20708.431	-0.123
d	169.503°	1.324	1.331	-20708.438	-0.324
e	171.694°	1.338	1.345	-20708.438	-0.328

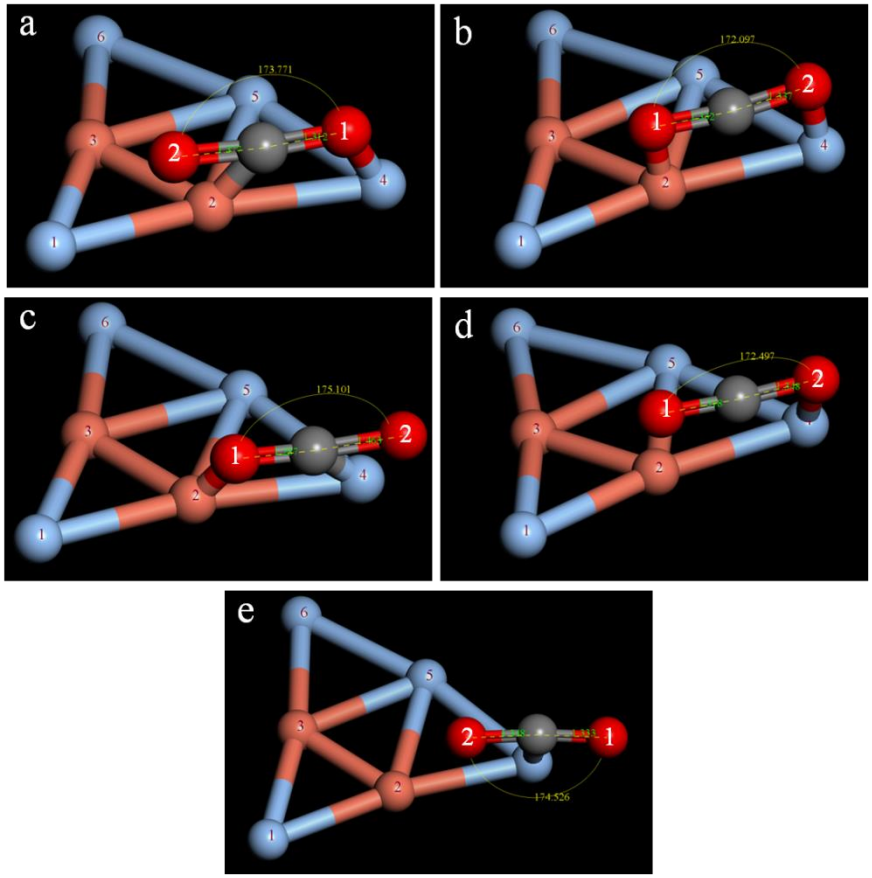

Figure S15. The isomers of the Cu_2Ag_4-CO_2 adsorption structure.

Table S13. Bond length, bond angle and energy of Cu_2Ag_4-CO_2 structure.

isomers	∠O1CO2/°	$d_{C\text{-}O1}$/ Å	$d_{C\text{-}O2}$/ Å	$E_{CuAg\text{-}CO2}$/ Ha	E_{obs} / eV
a	173.771°	1.312	1.377	-24267.688	-0.085
b	172.097°	1.332	1.337	-24267.689	-0.122
c	171.101°	1.287	1.463	-24267.677	0.208
d	172.497°	1.318	1.348	-24267.689	-0.113
e	174.526°	1.333	1.348	-24267.690	-0.151

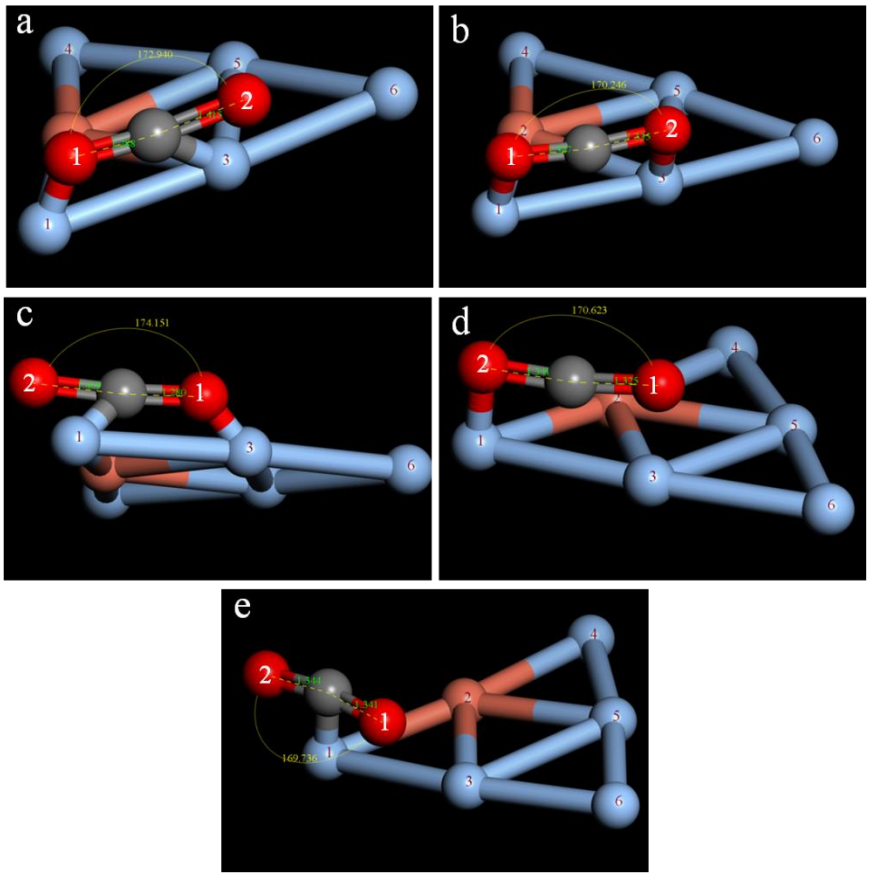

Figure S16. The isomers of the Cu_1Ag_5-CO_2 adsorption structure.

Table S14. Bond length, bond angle and energy of Cu_1Ag_5-CO_2 structure.

isomers	∠O1CO2/°	$d_{C\text{-}O1}$/ Å	$d_{C\text{-}O2}$/ Å	$E_{CuAg\text{-}CO2}$/ Ha	E_{obs} / eV
a	172.940°	1.288	1.415	-27826.950	-0.164
b	170.246°	1.327	1.335	-27826.950	-0.159
c	174.151°	1.280	1.409	-27826.948	-0.106
d	170.623°	1.325	1.341	-27826.947	-0.032
e	169.736°	1.341	1.344	-27826.949	-0.127

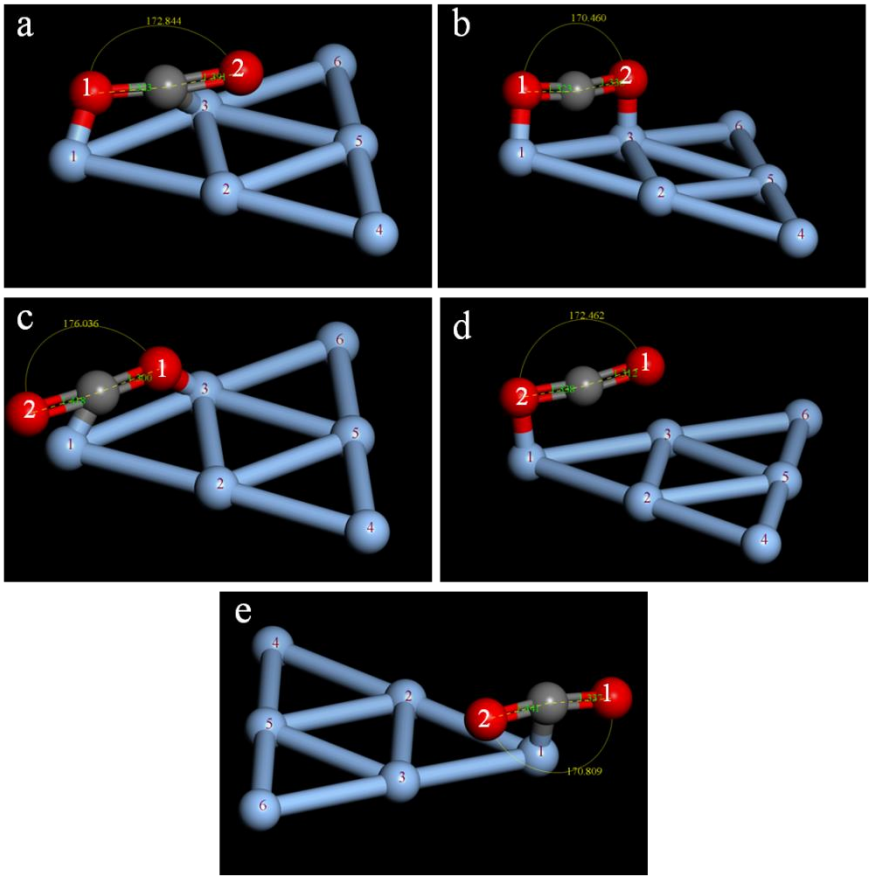

Figure S17. The isomers of the Ag_6-CO_2 adsorption structure.

Table S15. Bond length, bond angle and energy of Ag_6-CO_2 structure.

isomers	∠O1CO2/°	$d_{C\text{-}O1}$/ Å	$d_{C\text{-}O2}$/ Å	$E_{CuAg\text{-}CO2}$/ Ha	E_{obs} / eV
a	172.844°	1.323	1.391	-31386.212	-0.174
b	170.460°	1.320	1.333	-31386.211	-0.156
c	176.036°	1.300	1.418	-31386.211	-0.153
d	172.462°	1.312	1.338	-31386.212	-0.161
e	170.809°	1.337	1.341	-31386.211	-0.146

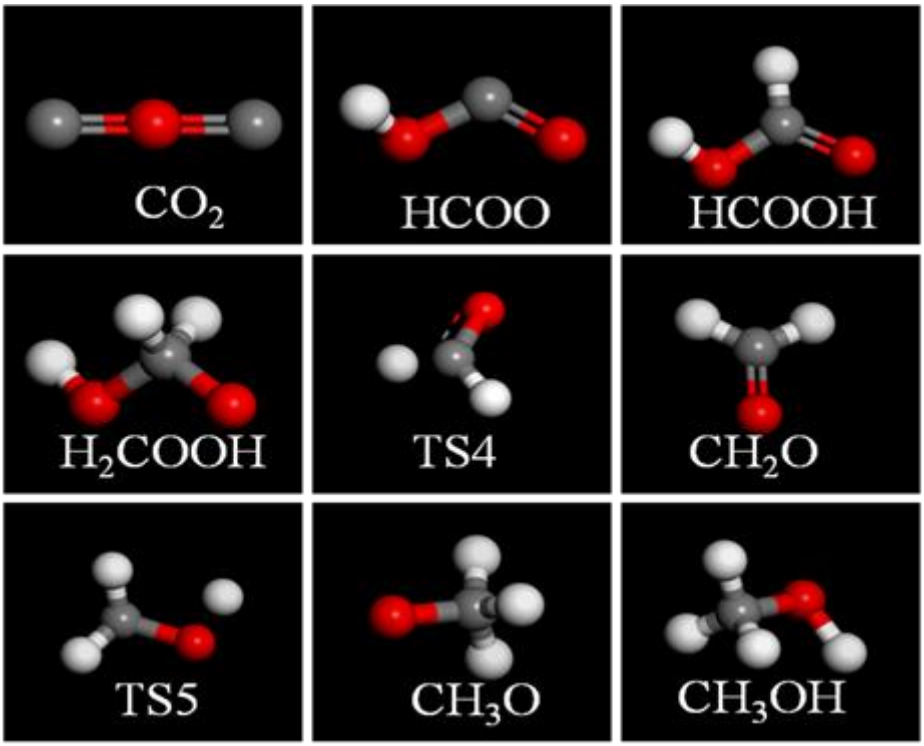

Figure S18. The optimized configuration of the monomer structure in the CO_2 to CH_3OH route.

Table S16. Gibbs free energy table of monomers for the hydrogenation of CO_2 to CH_3OH.

intermediate	Δ*G*/eV
CO_2^*+6H*	0
HCOO*+5H*	177.037
HCOOH*+4H*	218.916
H_2COOH*+3H*	244.005
TS4+H_2O+2H*	154.506
CH_2O*+H_2O+2H*	266.481
TS5+H_2O+H*	275.869
CH_3O*+H_2O+H*	353.449
CH_3OH+H_2O	389.422

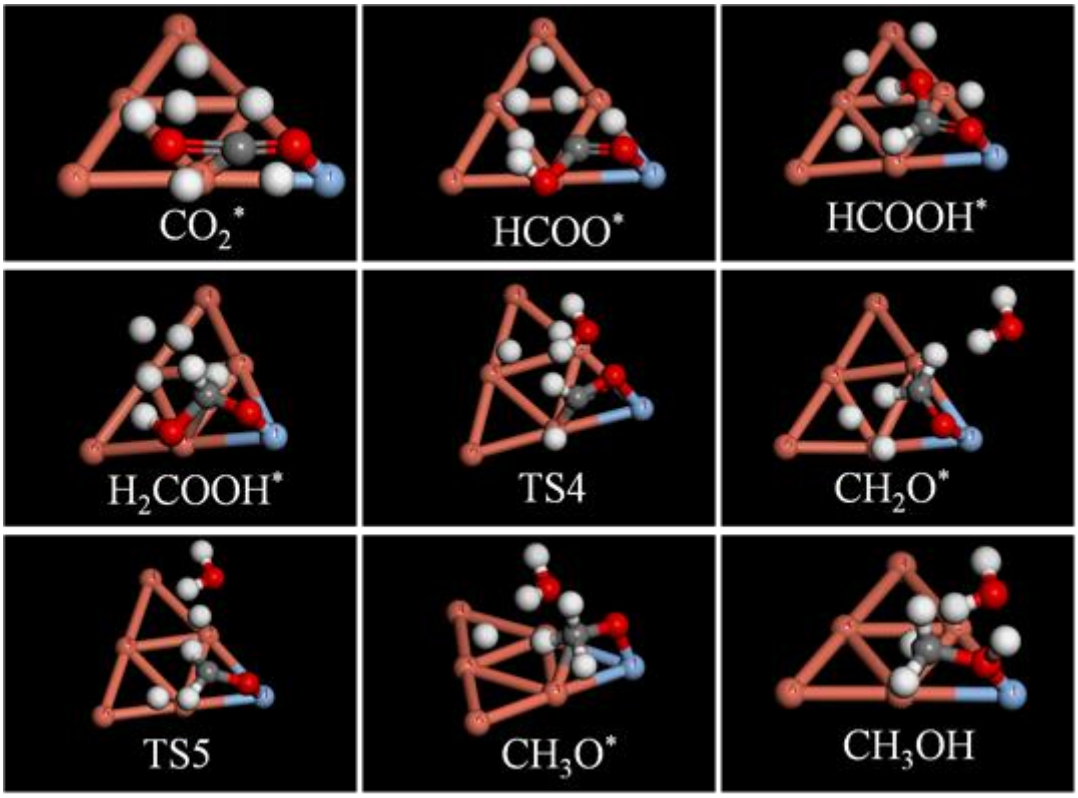

Figure S19. The path monomer adsorbed on Cu_5Ag_1 cluster.

Table S17. Gibbs free energy table of Cu_5Ag_1 clusters catalyzed by CO_2 hydrogenation to CH_3OH monomer.

intermediate	Δ*G*/eV
CO_2^*+6H*	0
HCOO* +5H*	-115.567
HCOOH*+4H*	-23.783
H_2COOH^* +3H*	168.928
TS4+H_2O+2H*	56.573
CH_2O^*+H_2O+2H*	-88.546
TS5+H_2O+H*	-31.103
CH_3O^* +H_2O+H*	73.580
CH_3OH+H_2O	84.709

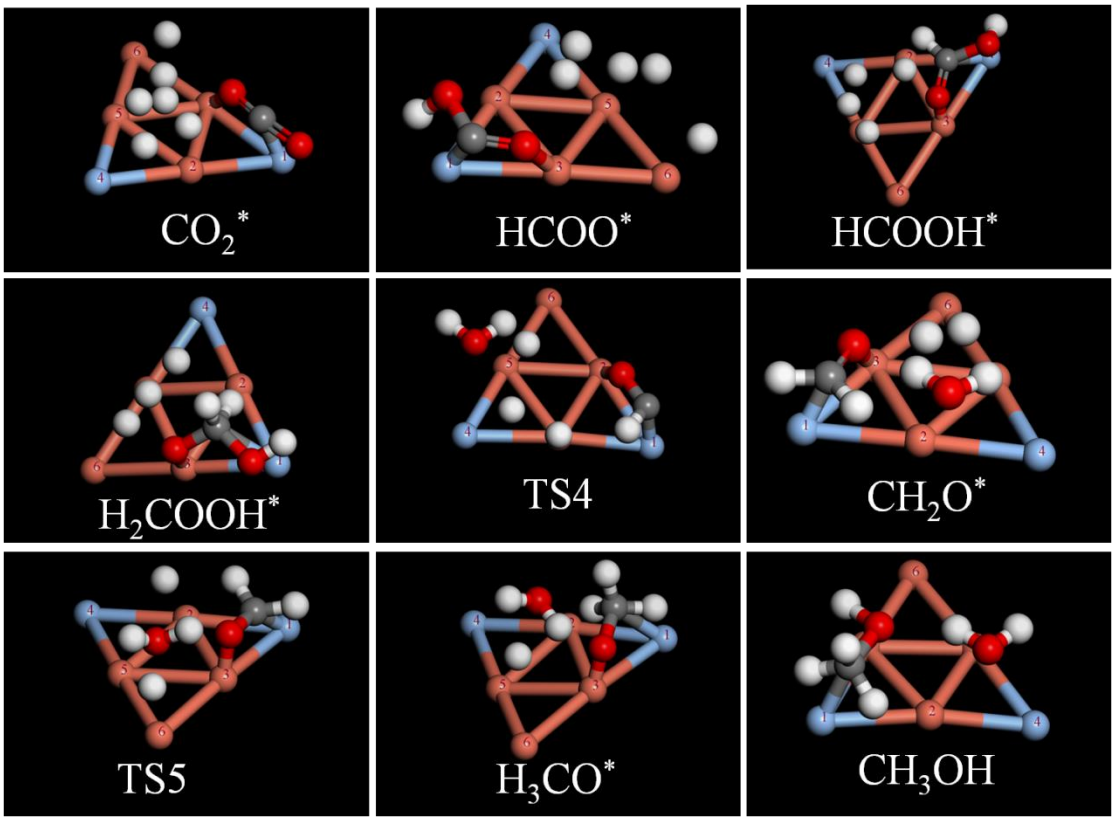

Figure S20. The path monomer adsorbed on Cu_4Ag_2 cluster.

Table S18. Gibbs free energy table of Cu_4Ag_2 clusters catalyzed by CO_2 hydrogenation to CH_3OH monomer.

intermediate	Δ*G*/eV
CO_2^*+6H*	0
HCOO* +5H*	-236.277
HCOOH*+4H*	209.065
H_2COOH^* +3H*	152.493
TS4+H_2O+2H*	-169.364
CH_2O^*+H_2O+2H*	205.854
TS5+H_2O+H*	194.099
CH_3O^* +H_2O+H*	324.822
CH_3OH+H_2O	129.553

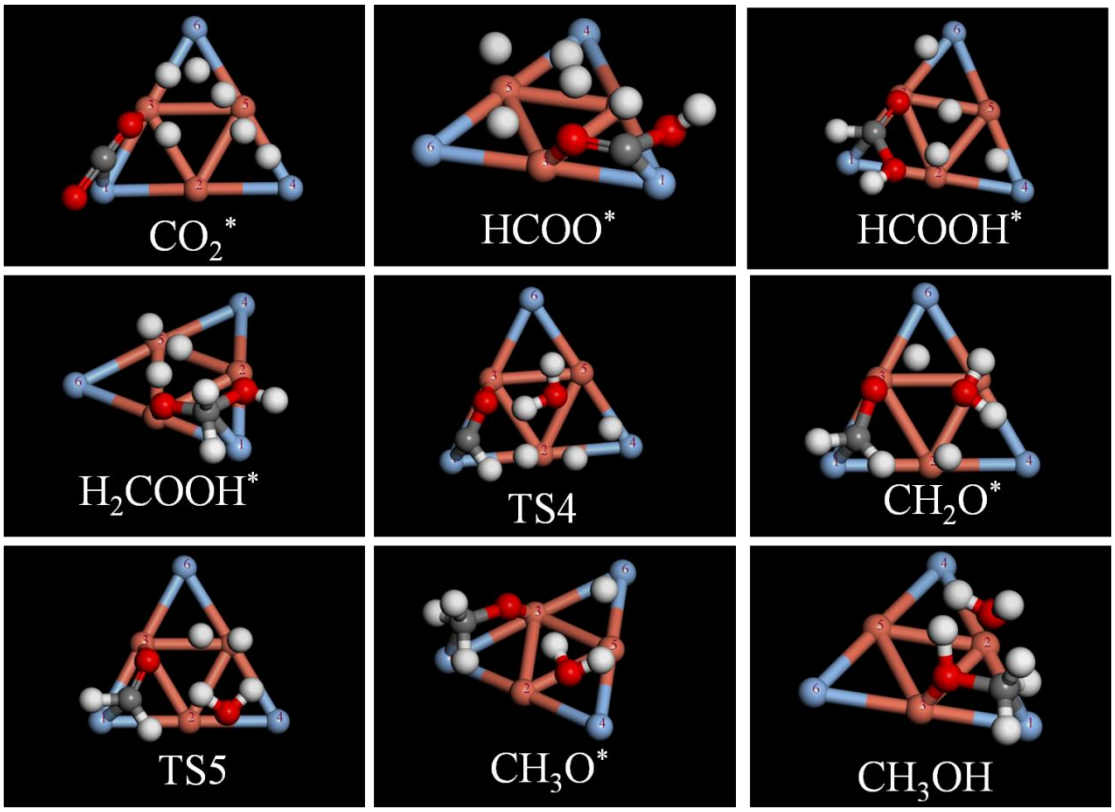

Figure S21. The path monomer adsorbed on Cu_3Ag_3 cluster.

Table S19. Gibbs free energy table of Cu_3Ag_3 clusters catalyzed by CO_2 hydrogenation to CH_3OH monomer.

intermediate	Δ*G*/eV
CO_2^*+6H*	0
HCOO* +5H*	45.280
HCOOH*+4H*	198.834
H_2COOH^* +3H*	97.607
TS4+H_2O+2H*	177.282
CH_2O^*+H_2O+2H*	183.813
TS5+H_2O+H*	208.657
CH_3O^* +H_2O+H*	122.342
CH_3OH+H_2O	236.630

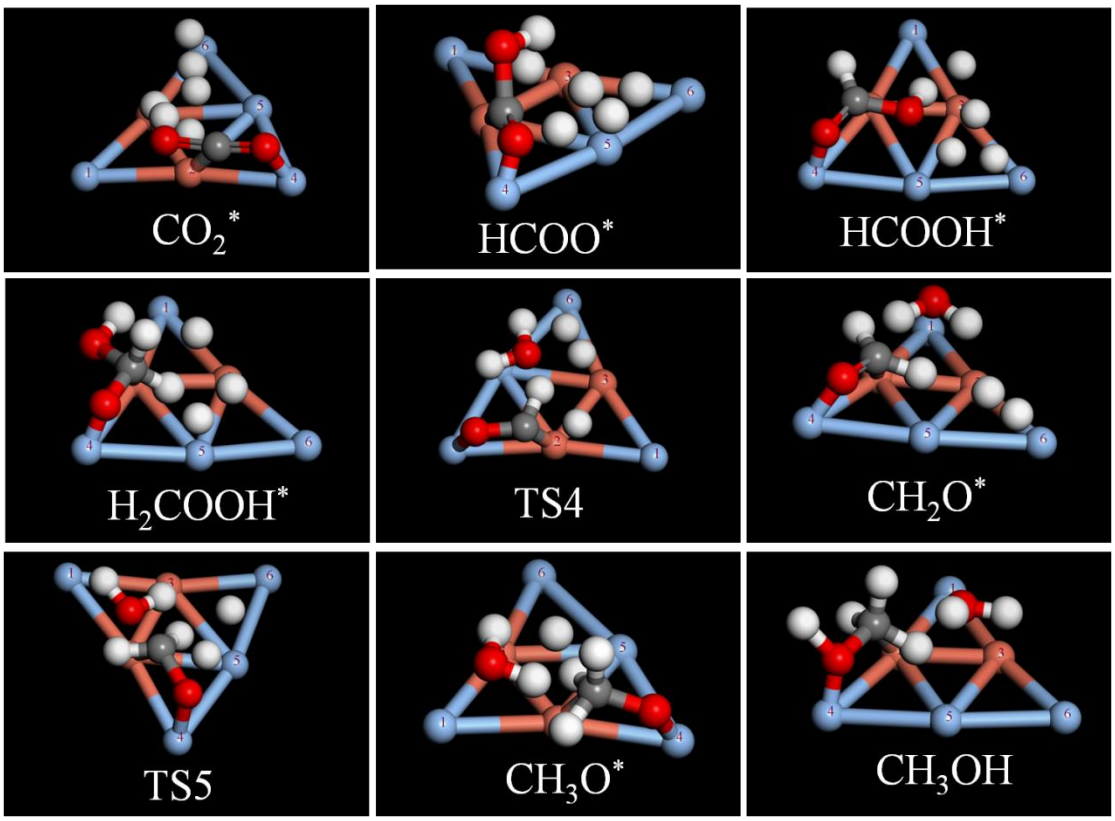

Figure S22. The path monomer adsorbed on Cu_2Ag_4 cluster.

Table S20. Gibbs free energy table of Cu_2Ag_4 clusters catalyzed by CO_2 hydrogenation to CH_3OH monomer.

intermediate	ΔG/eV
$CO_2^*+6H^*$	0
$HCOO^*+5H^*$	-433.097
$HCOOH^*+4H^*$	-549.779
$H_2COOH^*+3H^*$	-618.951
$TS4+H_2O+2H^*$	-603.358
$CH_2O^*+H_2O+2H^*$	-525.262
$TS5+H_2O+H^*$	-629.318
$CH_3O^*+H_2O+H^*$	-457.777
CH_3OH+H_2O	-501.452

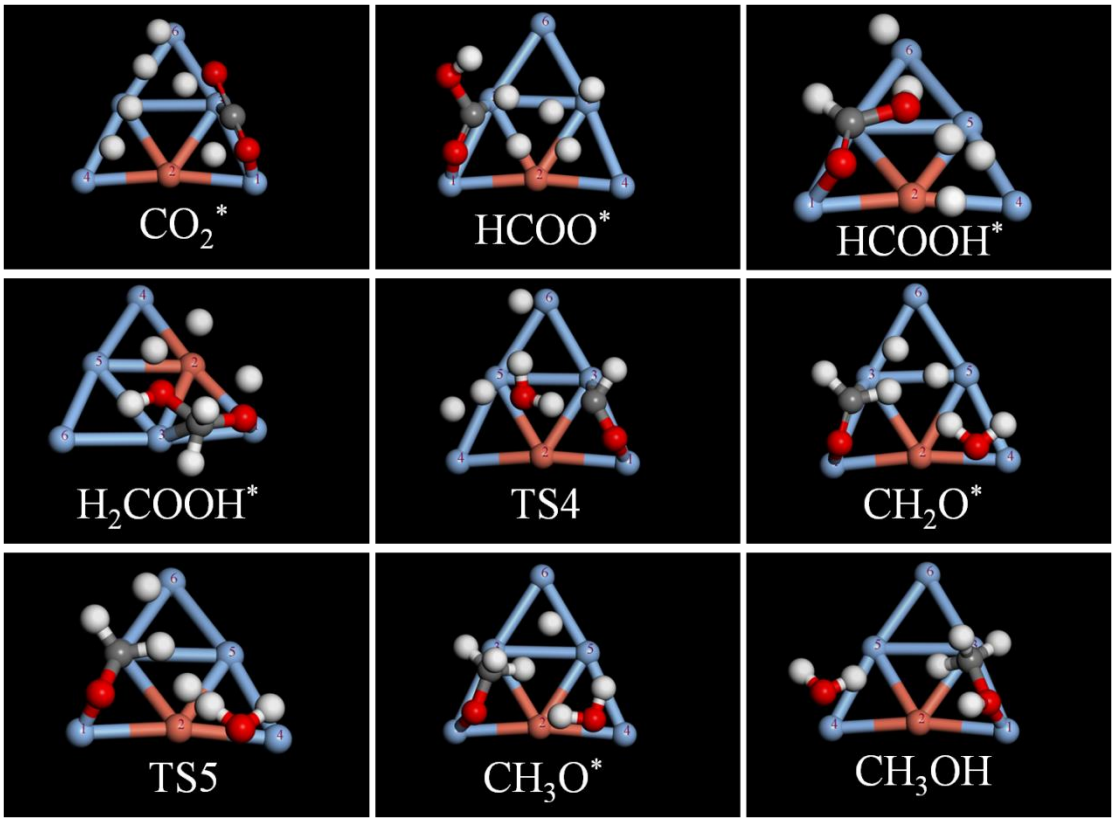

Figure S23. The path monomer adsorbed on Cu_1Ag_5 cluster.

Table S21. Gibbs free energy table of Cu_1Ag_5 clusters catalyzed by CO_2 hydrogenation to CH_3OH monomer.

intermediate	ΔG/eV
CO_2^*+6H*	0
HCOO* +5H*	-173.690
HCOOH*+4H*	-332.034
H_2COOH^* +3H*	-144.901
TS4+H_2O+2H*	-73.743
CH_2O^*+H_2O+2H*	-106.369
TS5+H_2O+H*	116.247
CH_3O^* +H_2O+H*	-11.783
CH_3OH+H_2O	23.456

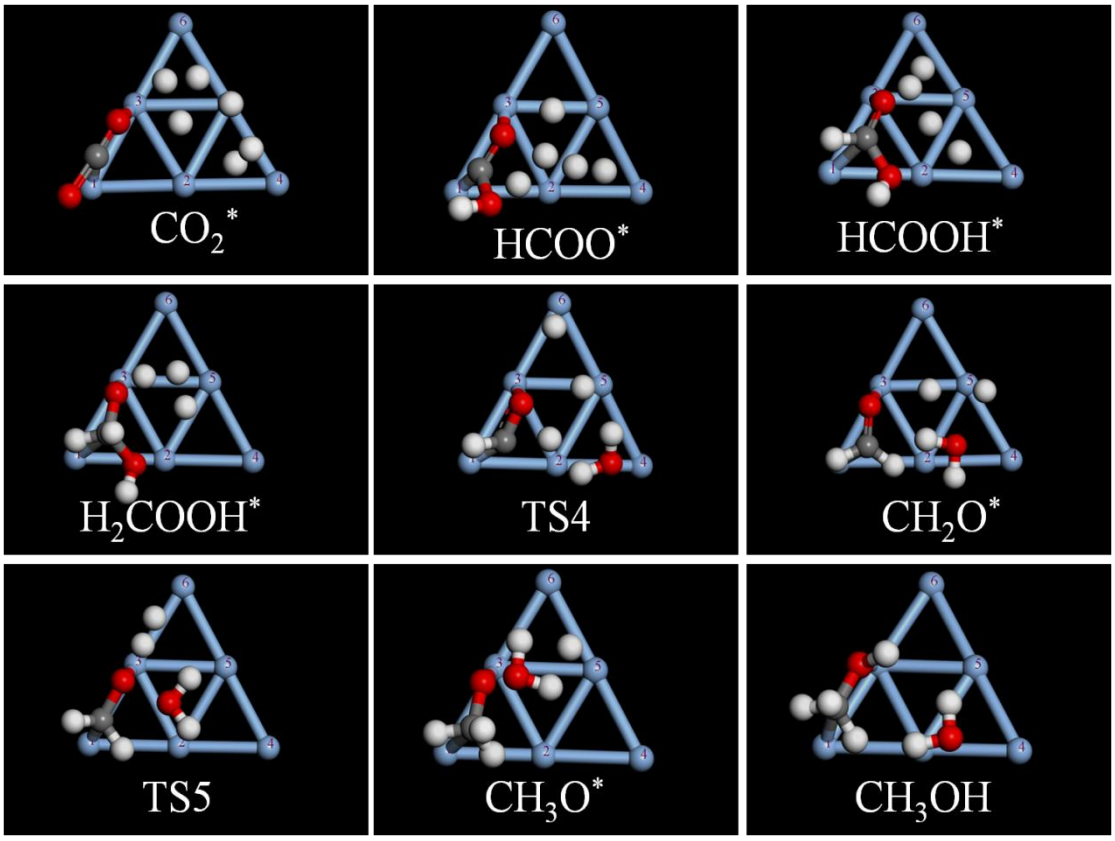

Figure S24. The path monomer adsorbed on Ag_6 cluster.

Table S22. Gibbs free energy table of Ag_6 clusters catalyzed by CO_2 hydrogenation to CH_3OH monomer.

intermediate	ΔG/eV
CO_2^*+6H*	0
HCOO* +5H*	390.348
HCOOH*+4H*	326.754
H2COOH* +3H*	483.873
TS4+H2O+2H*	537.017
CH2O*+H2O+2H*	591.712
TS5+H2O+H*	528.962
CH3O* +H2O+H*	510.132
CH3OH+H2O	482.893

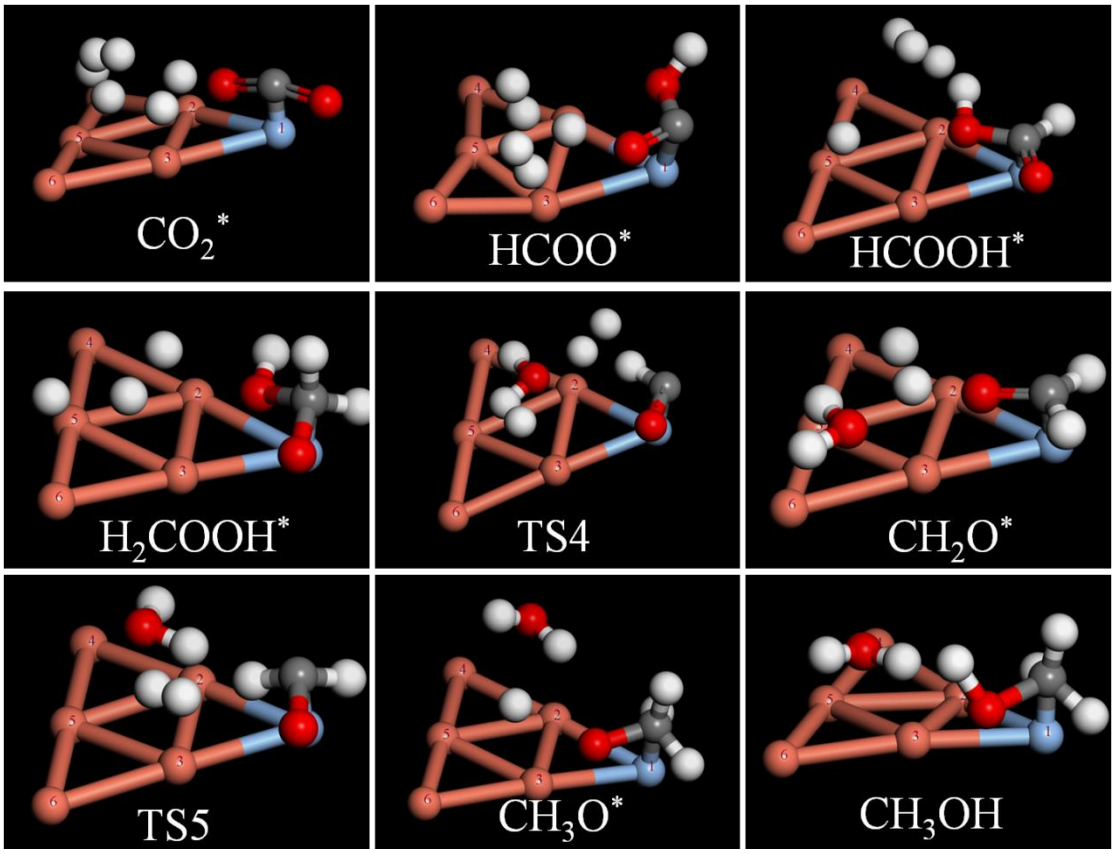

Figure S25. The path monomer adsorbed on Cu_5Ag_1 cluster.

Table S23. Gibbs free energy table of Cu_5Ag_1 clusters catalyzed by CO_2 hydrogenation to CH_3OH monomer.

intermediate	ΔG/eV
$CO_2^*+6H^*$	0
$HCOO^*+5H^*$	-187.922
$HCOOH^*+4H^*$	-118.152
$H_2COOH^*+3H^*$	134.016
$TS4+H_2O+2H^*$	-146.860
$CH_2O^*+H_2O+2H^*$	75.240
$TS5+H_2O+H^*$	123.948
$CH_3O^*+H_2O+H^*$	140.438
CH_3OH+H_2O	194.262

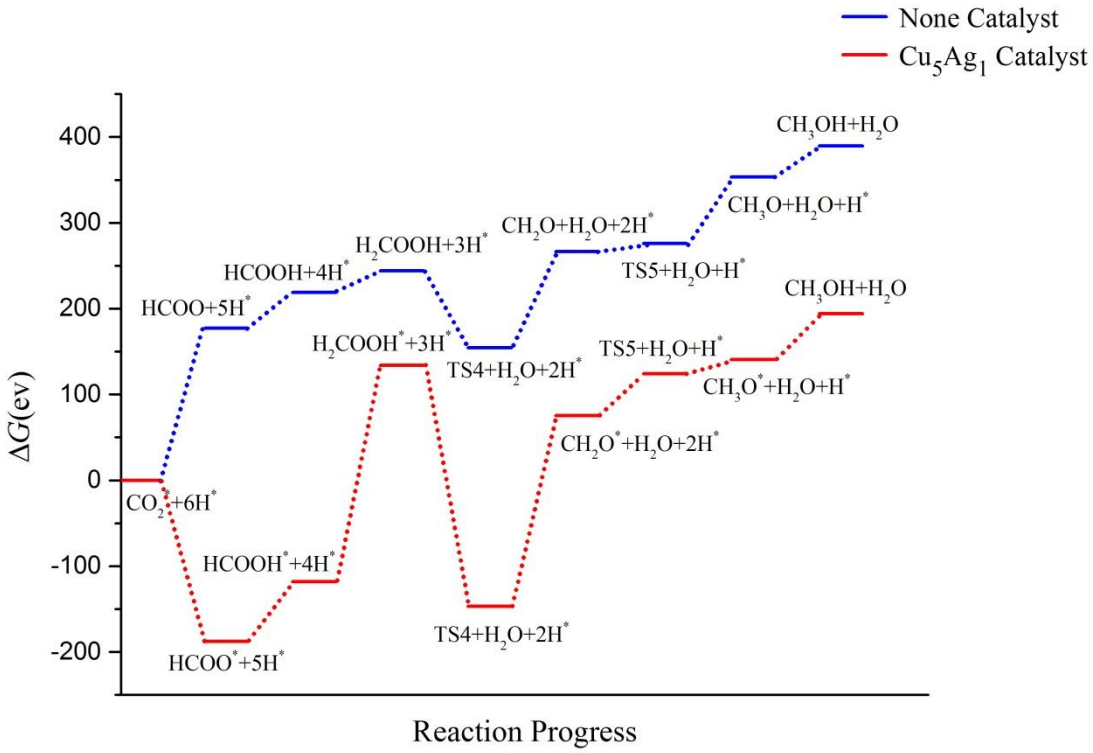

Figure S26. The path diagram of CO_2 hydrogenation reduction to CH_3OH catalyzed by Cu_5Ag_1 cluster.

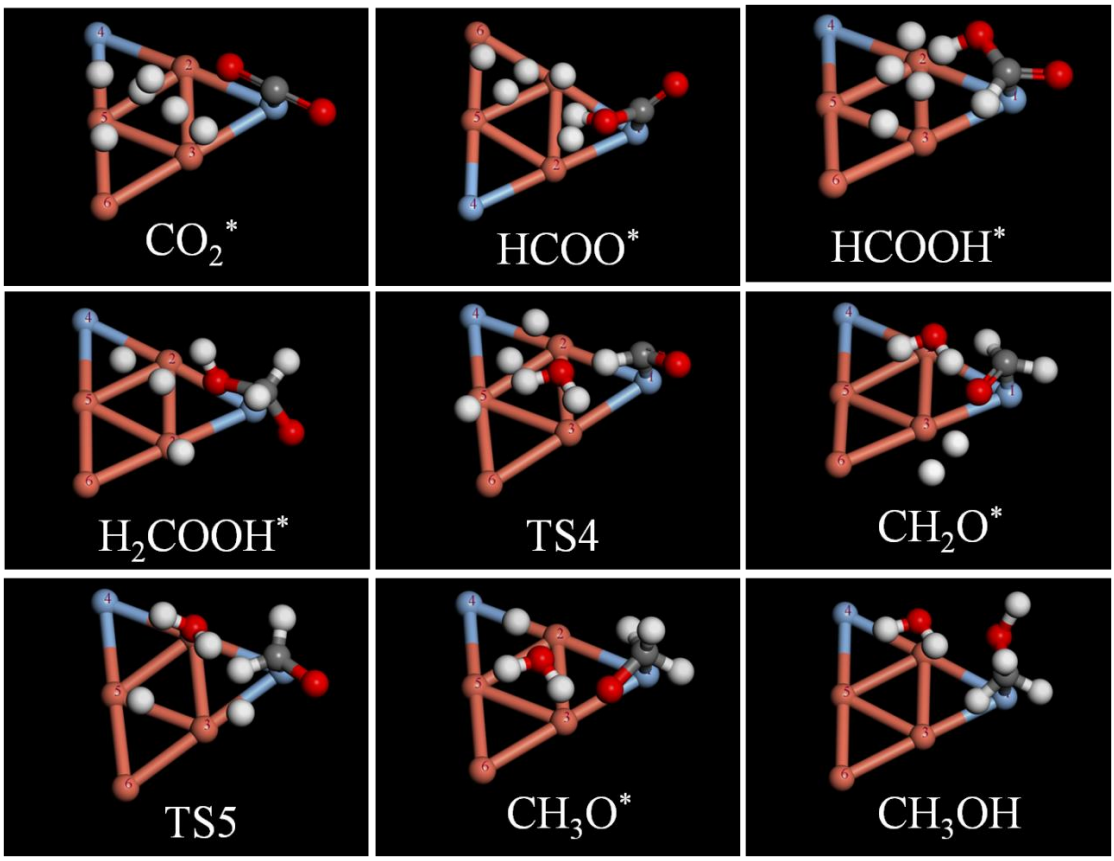

Figure S27. The path monomer adsorbed on Cu_4Ag_2 cluster.

Table S24. Gibbs free energy table of Cu_4Ag_2 clusters catalyzed by CO_2 hydrogenation to CH_3OH monomer.

intermediate	Δ*G*/eV
$CO_2^*+6H^*$	0
$HCOO^*+5H^*$	-147.703
$HCOOH^*+4H^*$	28.164
$H_2COOH^*+3H^*$	207.759
$TS4+H_2O+2H^*$	102.260
$CH_2O^*+H_2O+2H^*$	84.355
$TS5+H_2O+H^*$	287.706
$CH_3O^*+H_2O+H^*$	331.952
CH_3OH+H_2O	266.617

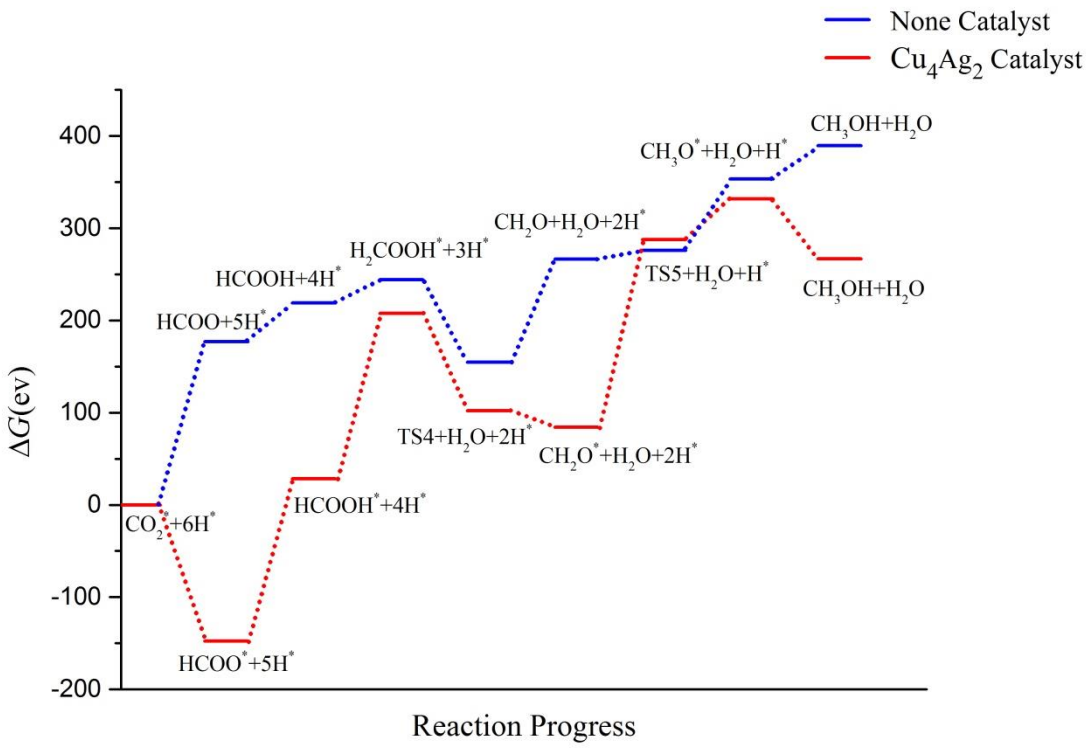

Figure S28. The path diagram of CO_2 hydrogenation reduction to CH_3OH catalyzed by Cu_4Ag_2 cluster.

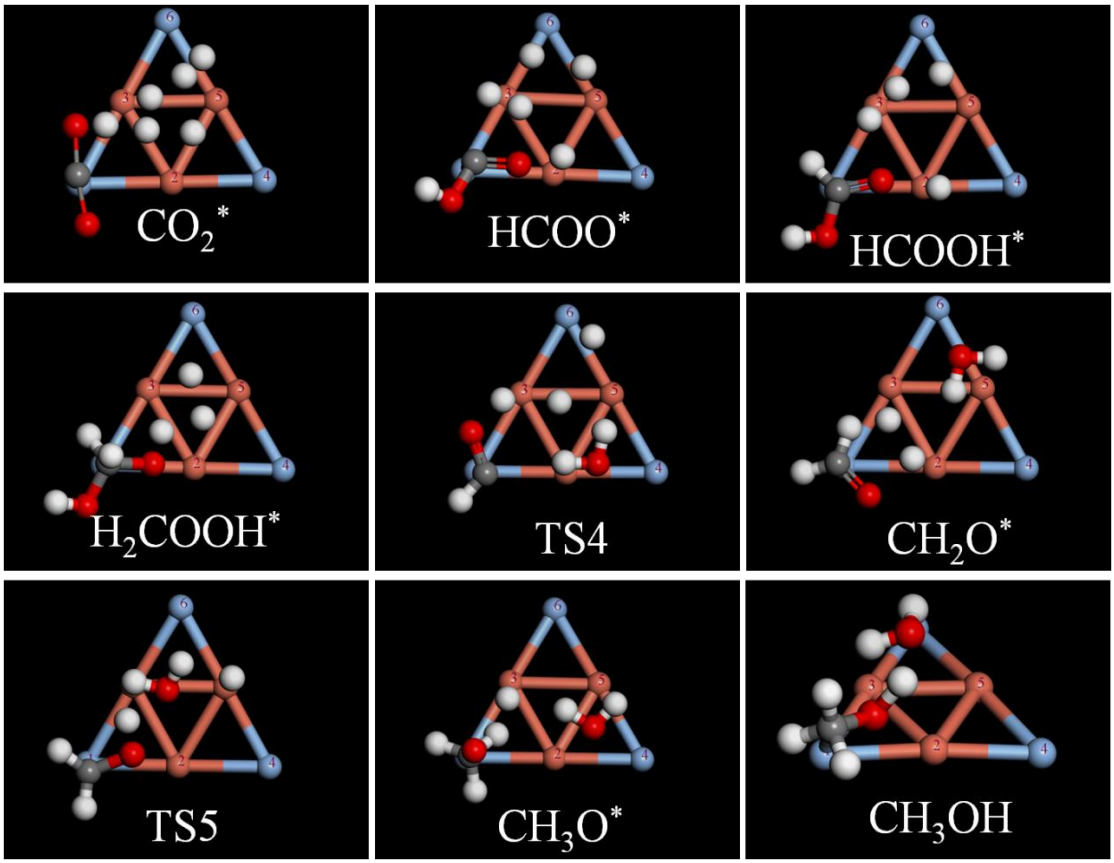

Figure S29. The path monomer adsorbed on Cu_3Ag_3 cluster.

Table S25. Gibbs free energy table of Cu_3Ag_3 clusters catalyzed by CO_2 hydrogenation to CH_3OH monomer.

intermediate	Δ*G*/eV
$CO_2^*+6H^*$	0
$HCOO^*+5H^*$	-79.430
$HCOOH^*+4H^*$	-286.019
$H_2COOH^*+3H^*$	-5.116
$TS4+H_2O+2H^*$	-184.983
$CH_2O^*+H_2O+2H^*$	-41.661
$TS5+H_2O+H^*$	129.281
$CH_3O^*+H_2O+H^*$	-40.463
CH_3OH+H_2O	242.399

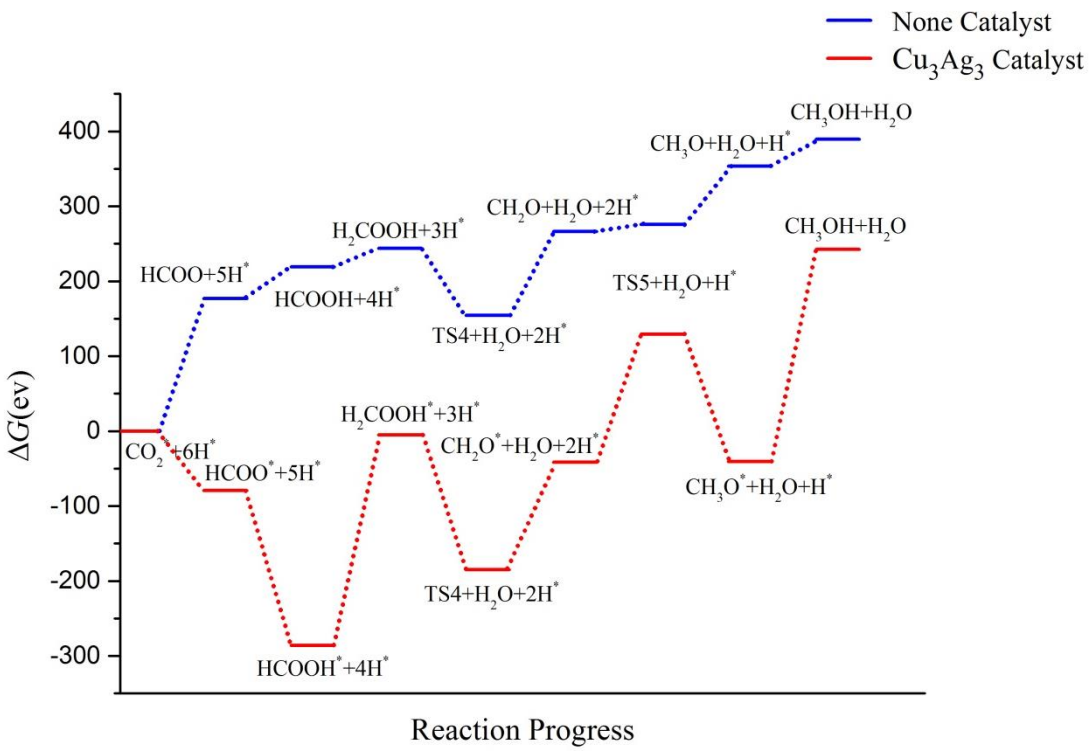

Figure S30. The path diagram of CO_2 hydrogenation reduction to CH_3OH catalyzed by Cu_3Ag_3 cluster.

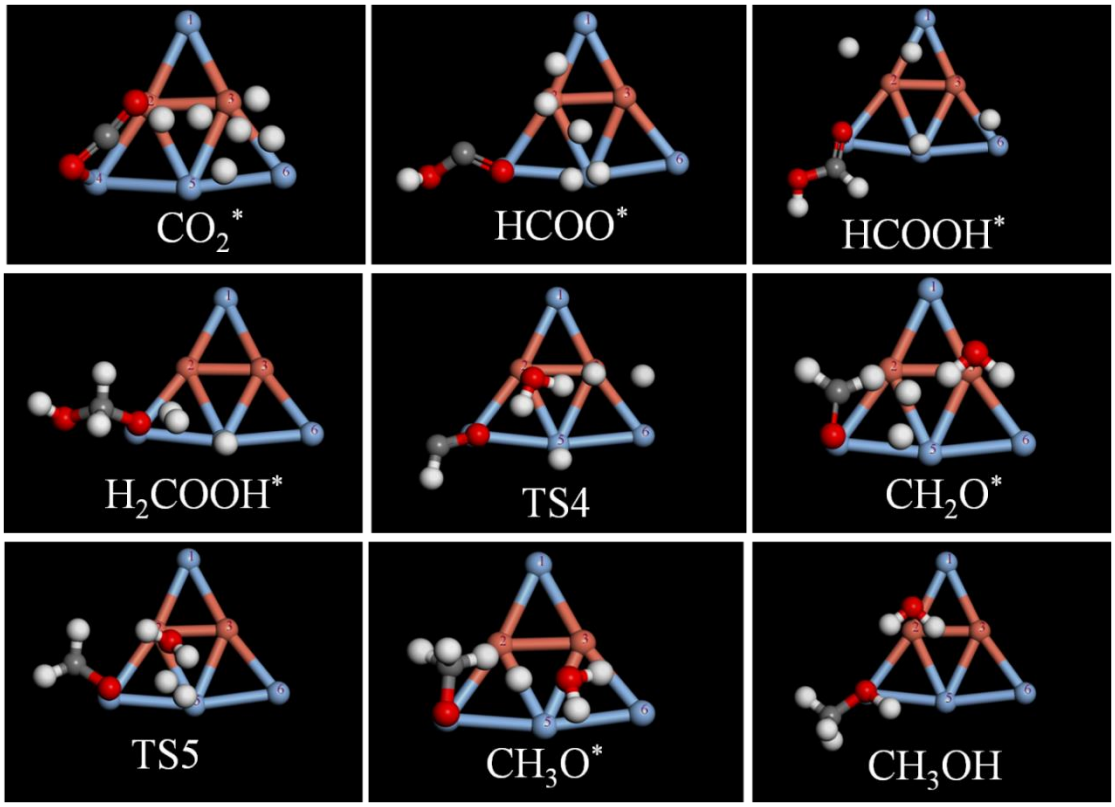

Figure S31. The path monomer adsorbed on Cu_2Ag_4 cluster.

Table S26. Gibbs free energy table of Cu_2Ag_4 clusters catalyzed by CO_2 hydrogenation to CH_3OH monomer.

intermediate	Δ*G*/eV
CO_2^*+6H*	0
HCOO* +5H*	-370.048
HCOOH*+4H*	-91.321
H_2COOH^* +3H*	72.273
TS4+H_2O+2H*	-43.429
CH_2O^*+H_2O+2H*	-24.844
TS5+H_2O+H*	140.329
CH_3O^* +H_2O+H*	59.130
CH_3OH+H_2O	7.347

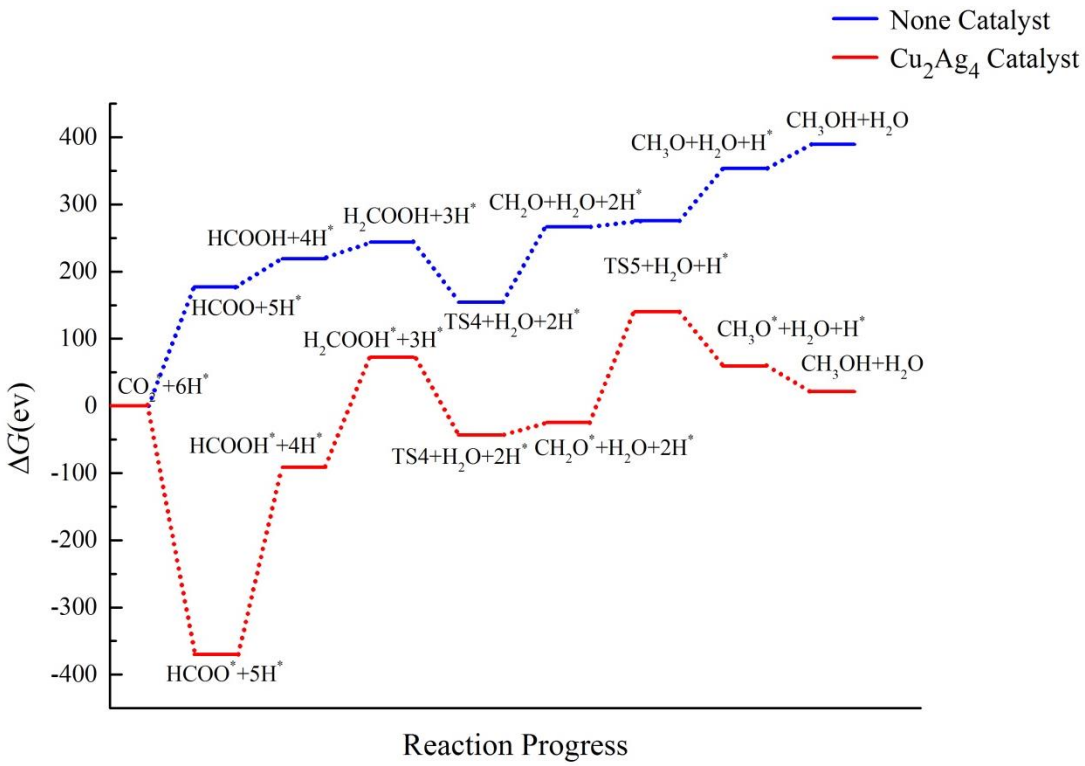

Figure S32. The path diagram of CO_2 hydrogenation reduction to CH_3OH catalyzed by Cu_2Ag_4 cluster.

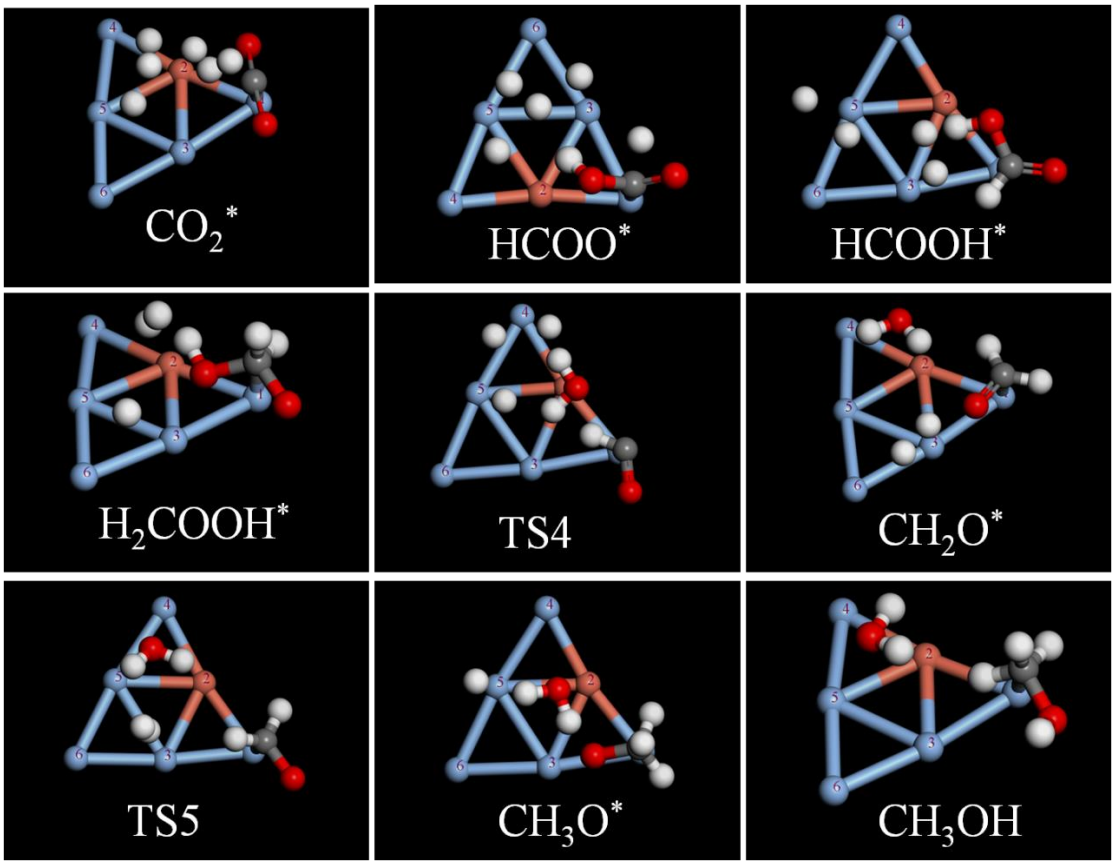

Figure S33. The path monomer adsorbed on Cu_1Ag_5 cluster.

Table S27. Gibbs free energy table of Cu_1Ag_5 clusters catalyzed by CO_2 hydrogenation to CH_3OH monomer.

intermediate	ΔG/eV
$CO_2^*+6H^*$	0
$HCOO^*+5H^*$	-272.577
$HCOOH^*+4H^*$	61.879
$H_2COOH^*+3H^*$	94.750
$TS4+H_2O+2H^*$	38.695
$CH_2O^*+H_2O+2H^*$	67.131
$TS5+H_2O+H^*$	177.146
$CH_3O^*+H_2O+H^*$	127.349
CH_3OH+H_2O	177.718

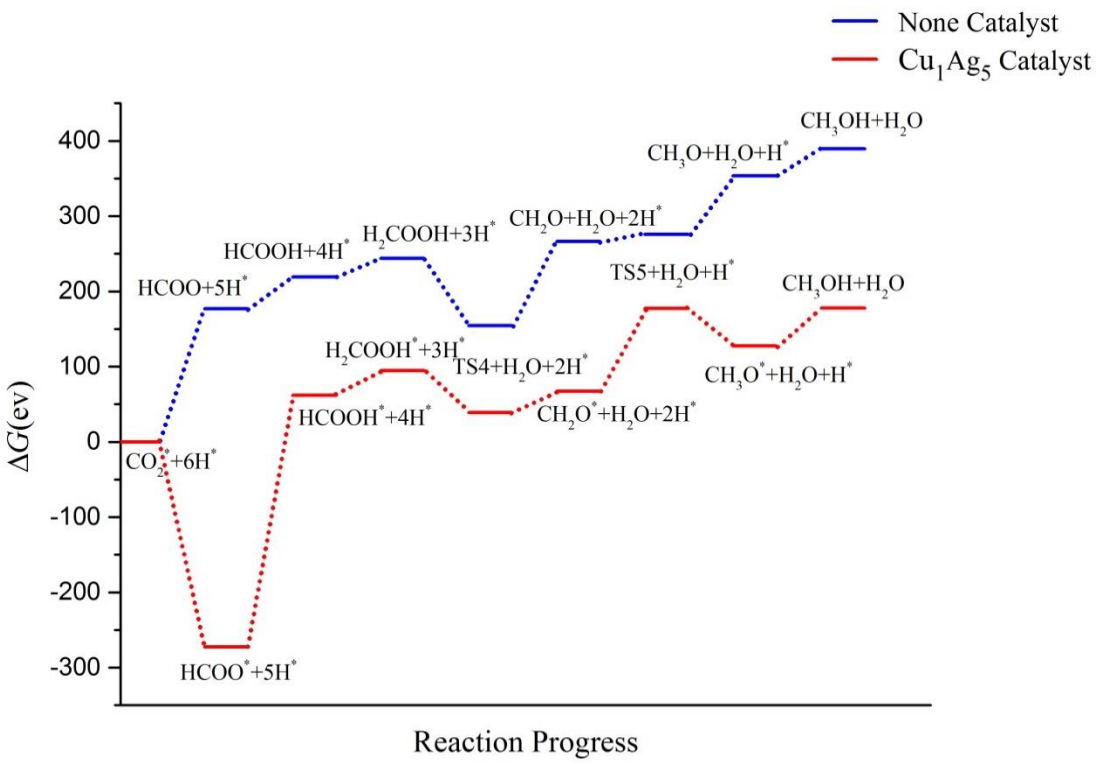

Figure S34. The path diagram of CO_2 hydrogenation reduction to CH_3OH catalyzed by Cu_1Ag_5 cluster.

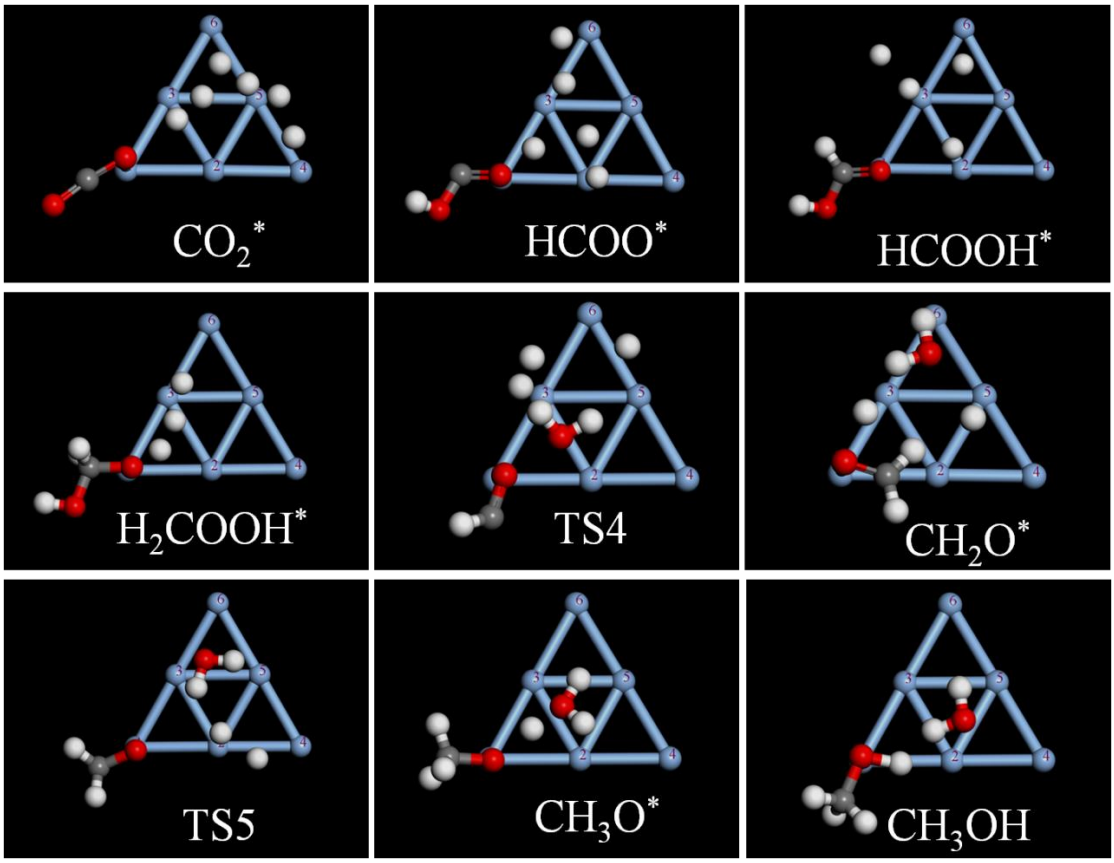

Figure S35. The path monomer adsorbed on Ag_6 cluster.

Table S28. Gibbs free energy table of Ag_6 clusters catalyzed by CO_2 hydrogenation to CH_3OH monomer.

intermediate	Δ*G*/eV
CO_2^*+6H*	0
HCOO* +5H*	156.275
HCOOH*+4H*	115.540
H_2COOH^* +3H*	369.585
TS4+H_2O+2H*	266.726
CH_2O^*+H_2O+2H*	391.953
TS5+H_2O+H*	517.615
CH_3O^* +H_2O+H*	331.598
CH_3OH+H_2O	499.329

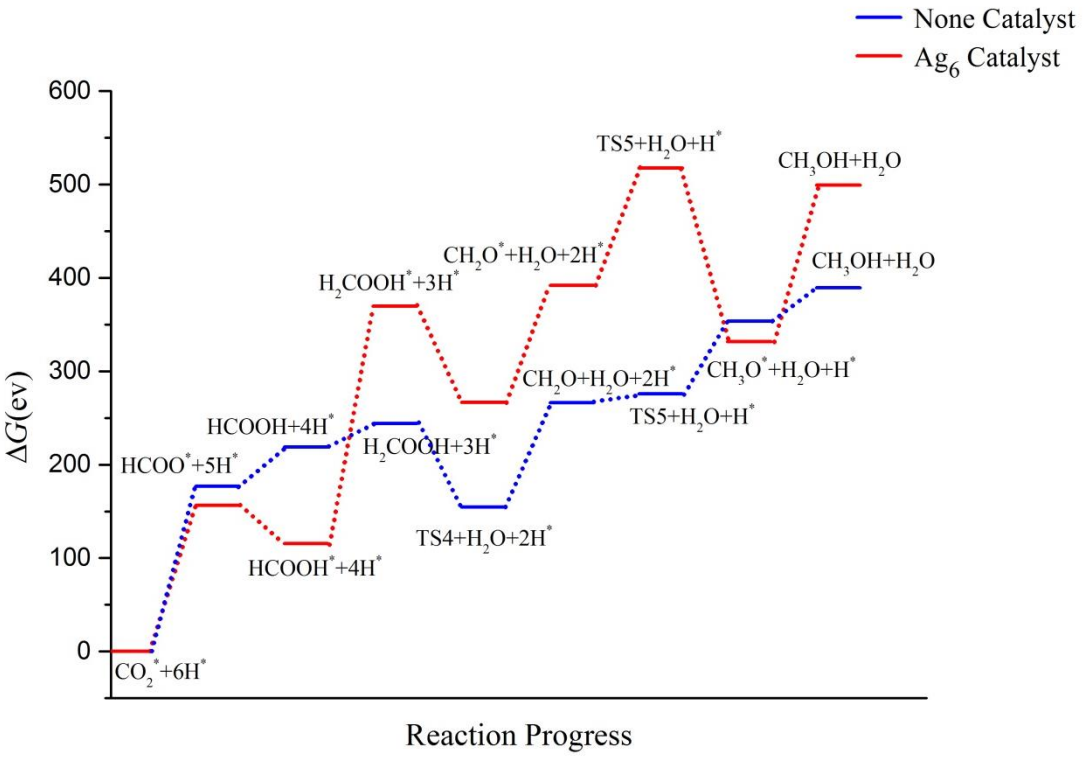

Figure S36. The path diagram of CO_2 hydrogenation reduction to CH_3OH catalyzed by Ag_6 cluster.

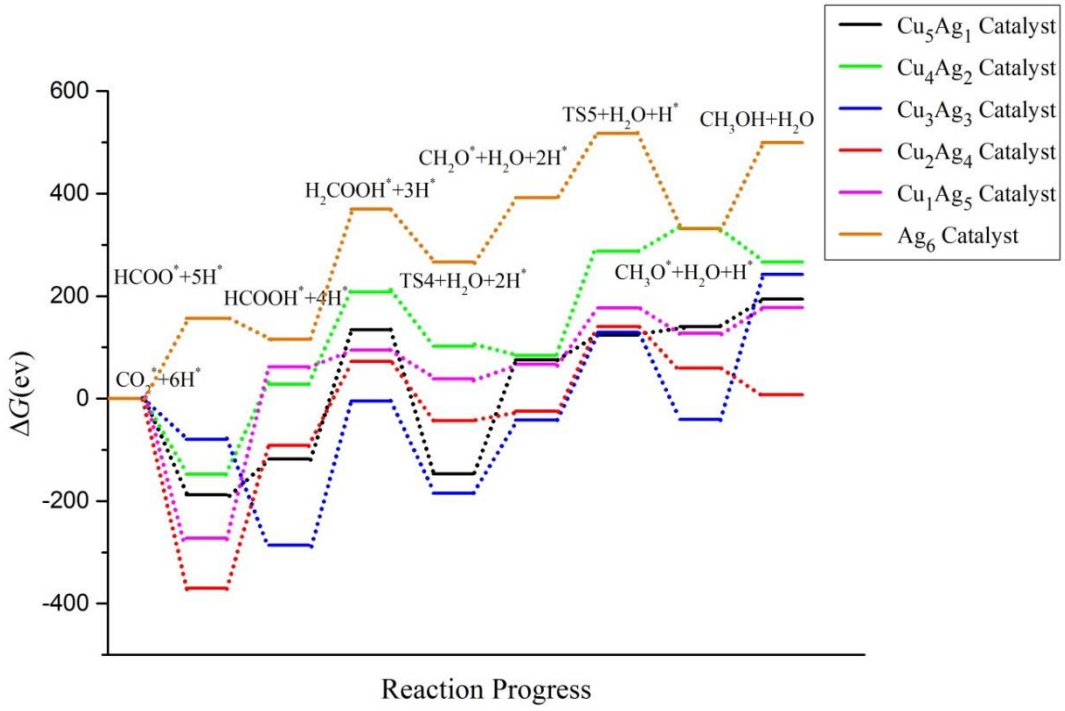

Figure S37. The path diagram of CO_2 hydrogenation reduction to CH_3OH catalyzed by CuAg clusters.